International Journal of Innovative
Computing, Information and Control
Volume 8, Number 12, December 2012

 ISSN 1349-4198
pp. 8147–8164

SCPS SOLUTION FOR HETEROGENEOUS NETWORKS FOR ISOLATED AREAS: A NOVEL DESIGN APPROACH

Satea Hikmat Alnajjar[1] and Fareq Malek[2]

[1]School of Computer and Communication Engineering
[2]School of Electrical System Engineering
Universiti Malaysia Perlis
Block A, Aras 1, Taman Seberang, Jaya Fasa 3, 02000 Kuala Perlis, Perlis, Malaysia
h.sat.nj@gmail.com; mfareq@unimap.edu.my

Received September 2011; revised January 2012

Abstract. *This research presents an innovative system that has capability to prove the technical feasibility and advantages of a joint radio frequency (RF) and free space optic (FSO) system with a synchronized self-trace directional between various deployments of mesh net nodes in the low space, with several factors driving this convergence. Sky mesh network utilizing aerial altitude platform system (AAPS) is driven via Wi-Fi and optical fiber combining the capacity of optical fiber networks with the deployment and mobility of wireless networks. Our proposed system is based on AAPS; however, this mechanism has encountered troubles in precariousness due to winds, a challenge that hinders network deployment due to loss of the line of sight (LoS). A smart communication platform system (SCPS) base station is proposed to overcome these restrictions. In this research, we experimentally simulate the SCPS, which provides more stability and accuracy in the transmission of RF and FSO. The proposed experimental simulation model considers the multi-hop wireless ad-hoc mesh networks and LoS between the mesh nodes in one unit with high performance and low weight and costs. Furthermore, fiber-optic cable (FOC) and FSO based quality of service (QoS) need to be enforced throughout the network in order to ensure that critical, latency-sensitive traffic is appropriately prioritized. This novel invention focuses on and evaluates the process approach of a coordinated transformations system based on linked FOC, FSO and RF in AAPS for a data rate of 1.25 Gps at 350 m.*

Keywords: Aerial altitude platform system (AAPS), Free space optics (FSO), Mesh network, Smart communication platform system (SCPS)

1. **Introduction.** A characteristic of the communications network is distinguished by being reliable, accessible, and easy to install. Wireless communications play a significant function in rural and disaster situations, since they provide decisive information to individuals and organizations, during natural or unnatural disasters, especially with communications infrastructure that has been disrupted and that requires immediate deployment of communications networks to implement the necessary relief. On the other hand, communication towers face the challenge of being expensive and not cost-effective for remote areas. In addition, satellite systems suffer from high infrastructure costs for each user via lack of infrastructure and a higher-priced installation compared with urban areas is the main obstacles in the construction of a wireless network in that the system will suit the needs of the rural community.

The demand for high-capacity services is bringing increasing challenges, particularly for transmission to the 'last mile'. In fact, the traditional techniques fail to provide access to these areas. Current approaches are trying to find appropriate means for the development and linking of networks.

The growing demand is to provide with high-efficiency services to meet the needs of users. Employment of the Aerial Altitude Platform System (AAPS) communication system is proposed to be carrying communications systems, which is our proposal to solve the problem of the 'last mile'. This proposal is not devoid of obstacles as well; the random motion due to strong winds causes deviation in the direction of the signal between the transmitter and receiving platforms. Another challenge to be considered is increasing demand for providing high efficiency services to enhance the performance.

One of the most promising applications is to employ an FSO with the wireless networks, to meet the growing need for high-speed services.

Previous studies in this area, particularly that use balloons for monitoring purposes, encountered problems in the instability of the images sent from the balloon to the ground stations because the violent vibrations were generated as a result of wind factors.

The last point has an influential role in the line of sight (LoS) transfer of a radio signal between the network nodes. With these limitations in the use of technology, AAPS is not effective especially in the mesh network, which requires several nodes for deployment. The situation requires the creation of an innovative mechanism to make a more stable transfer of signals between nodes. In this research, the proposed approach is a novel design of the detection method of an effective system that is able to sense environmental changes (self-movement system) and acts in accordance with the changes surrounding, where any resistance to change the direction of the antenna as a result of changes in the environmental factors, increases the reliability of the signal transmission between nodes in the network. Moreover, the choice of an effective approach that reduces these types of obstacles is presented and evaluated for all parts of this research.

Different communications technologies exist, and each of them with particular advantages and disadvantages, so by putting together a system combining those technologies would be exploiting the specific advantages of each technique.

This research is organized as follows. Section 2 describes the system design for the sky mesh network architecture. Section 3 describes the system design and simulation. Section 4 investigates the impairments wireless signals experience while being propagated over an optical link as well as the corresponding strategies to overcome these impairments. The

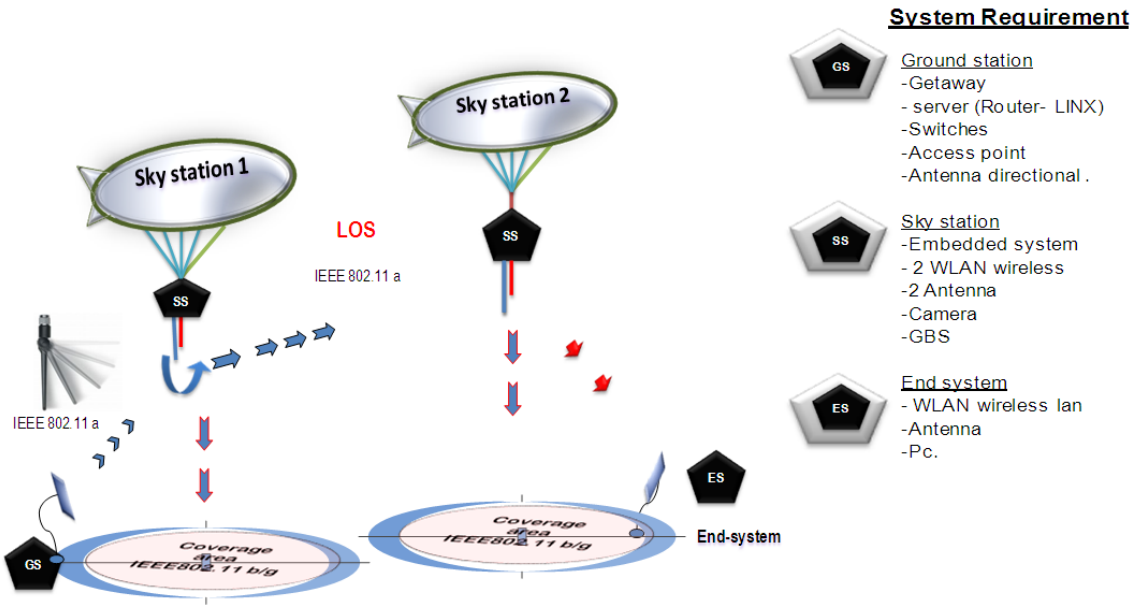

FIGURE 1. Aerial altitude platform system (AAPS) scenario topology

results and analysis appear in the Section 5. Finally, the conclusions are reported in Section 6.

The aim of this project is to present an innovative system that has the capability of adapting to environmental conditions that affect the AAPS; on the other hand, it provides high-reliability Gigabit Ethernet to deploy in the high-capacity backbone network links between mesh nodes.

2. System Design for Sky Mesh Network Architecture.

2.1. AAPS network architecture cycles. The proposal that was drafted for implementation uses two platforms, the main stage sky station1 (SS1), as the root node, which in turn sends the transmission signal to the second node sky station (SS2), for the transfer of data packets to their destination, the End-System. This ensures the LoS between the dispatch and receipt nodes. To implement the required two cycles adopted, each cycle of the AAPS has two steps.

First, there is the radio frequency partition; the ground station (GS) connects to SS1, and SS1 connects to SS2 via the IEEE 802.11a. Then, in second step, SS1 and SS2 provide a coverage area to the ground by utilizing the IEEE 802.11x wireless standards.

Figure 2 illustrates the overall system design; Figure 2(A) represents the GS, which is considered gateway to provide services to the outside world via VSAT, DSL, or any other source obtainable, such as fiber optic cable. The scenario approach in this research is through the optical cable system. Figures 2(B) and 2(C) illustrate the payload balloon.

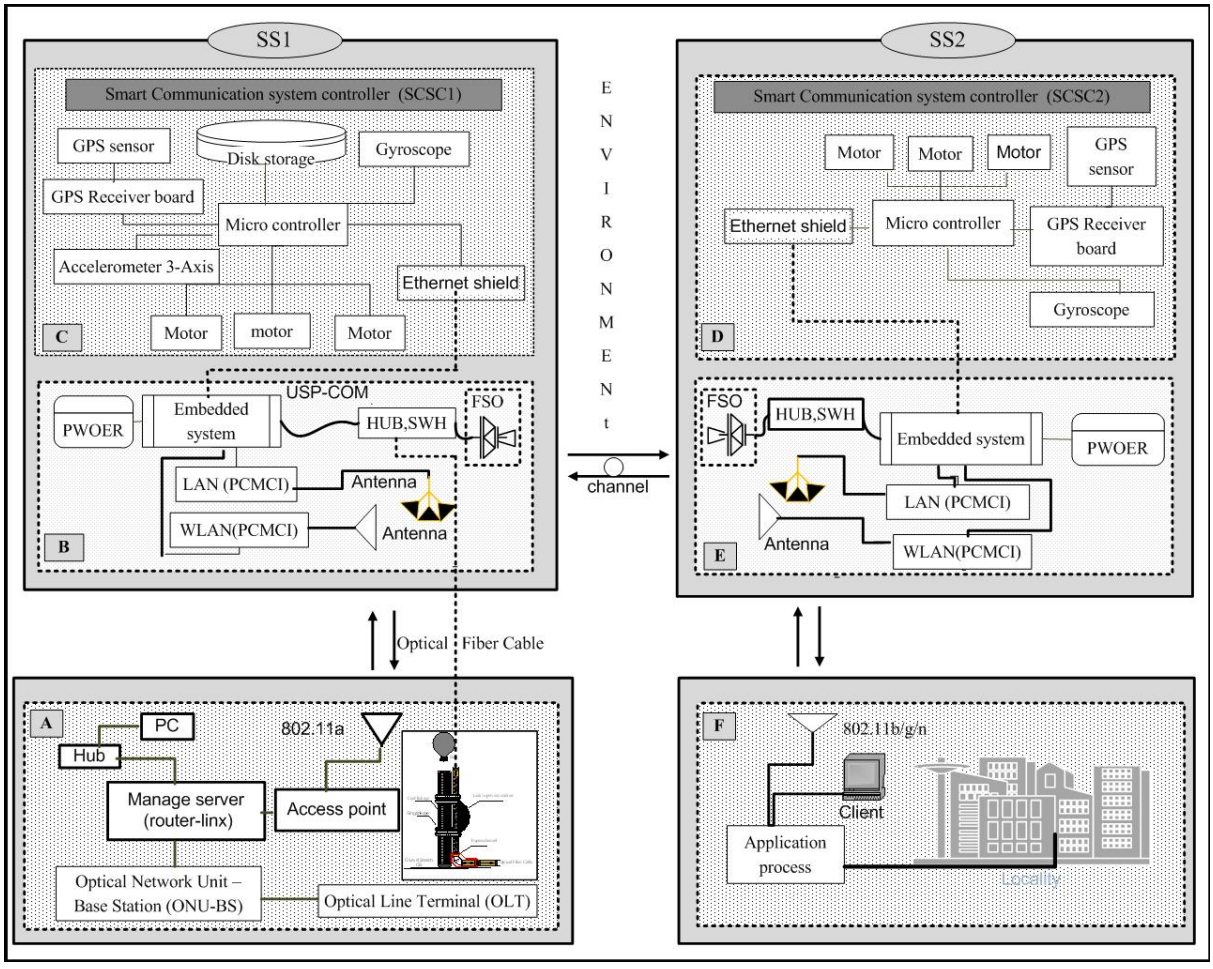

FIGURE 2. (AAPS) Physical architecture design

Figure 2(B) includes the embedded system optimized for routing signal functions between nodes; this device is associated with two wireless cards:

(1) Support IEEE 802.11a networking and (2) IEEE 802.11 b/g access points for a maximum range. It is also connected with two external high-power antennas for point-to-point links of frequency bands of 5.8 GHz and 2.4 GHz. The commercial product dual-radio EnRoute500 can serve as a Wi-Fi access point with a dedicated 802.11 b/g radio, an intra-network repeater and a router with a dedicated 802.11a mesh-enabled radio [4]; the specifications are used in communication systems for the AAPS, and correspond with this product.

The second-optical partition, the GS connects to SS1 via practical IEEE 802.3 optic fiber cables. In the second step, SS1 sends the signal to SS2 through the laser beam communication channel FSO. Figure 2(A) shows an additional unit to the source of the signal sent to the SS1. The ground station connects to SS1 using practical IEEE 802.3 fiber optics; physical connections are made between network nodes and infrastructure node devices (hubs, switches, routers) by various types of copper or fiber cable. Once the data arrives in SS1 system, Figures 2(B) and 2(E) illustrate the FSO system that installed in both systems SS1 and SS2. The FSO's only path ensures speed and reliability of communications between nodes, so the SS1 would divert the data to SS2 through the laser light communication channel to initiate a communication link between SS1 and SS2. Sky station2 also provides a broadcasting signal to the ground area coverage via the IEEE802.11. b/g standards to connect to the End-System users on the ground.

2.2. **Experimental setup for SCPS.** The physical nature of the transition waves in space requires the availability of a line of sight; the challenge in many applications in the absence of means to support mobile platforms, especially in the sky, this case applies to our current system. This situation requires the establishment of control systems to prevent the volatility factor due to wind. Reliability of the signal transmission between the mesh nodes depends on the constancy of the source transmitter, which is the focal point of discussion for this research. For the stability of the AAPS, the smart communication platform system (SCPS) is suggested to enhance the communication resources in areas that are desperately needed for this. SCPS is integrated systems that require an entire device to be attached to the tethered blimps. This system is characterized as light-weight, low in cost, and able to sense extraneous changes (self-directed) in the surrounding environment.

The SCPS components are illustrated in Figures 4 and 5 and consist of the following.

a) Sensitivity and control system platform. The Global Positioning System (GPS) is a space-based system that provides reliable location and time information for AAPS. GPS sensors with the board shield for the purpose of linking with the micro controller.
b) Embedded system hardware and personal computer memory card international (PCMCIA) – WAN and LAN that are shown in Figure 5, D2.
c) Figure 5 illustrates the dynamic part of the sub-platform with motors, designed to receive the signal that has been sent by the micro controller, and to organize the movement of the communication system (antennas and FSO) systems that have been installed in the platform.
d) Fiber optic physical connections link the network nodes to the nodes of the infrastructure devices (hubs, switches, routers).
e) Second-cycle optical partition's technology that provides bidirectional communication transfer rates for the Gigabit Ethernet, FSO system. It is capable of sending up to 1.25 Gbps of data. This system was installed on the basis of mobile axes, and controlled by the system SCSC, as shown in Figures 3 and 4.

f) Fiber optic cable proposed to link GS to SS1 in order to produce a gateway from the ground station to the sky station. Figure 3 illustrates the procedures of connection with the necessary requirements.
g) IP camera system works to survey the disaster area by using wireless network, to collect the information around the area [5].

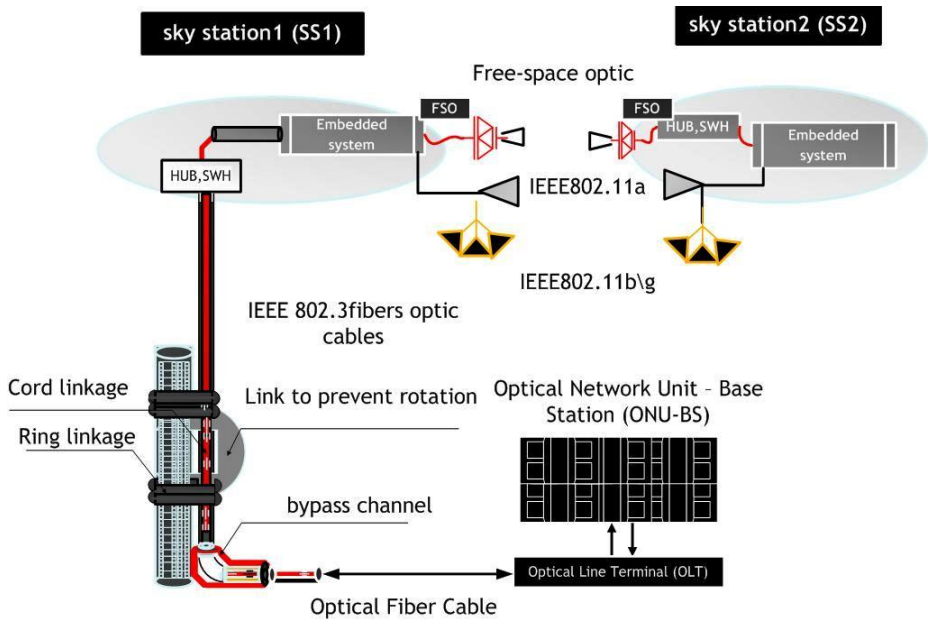

FIGURE 3. Fibers optic cable architecture design

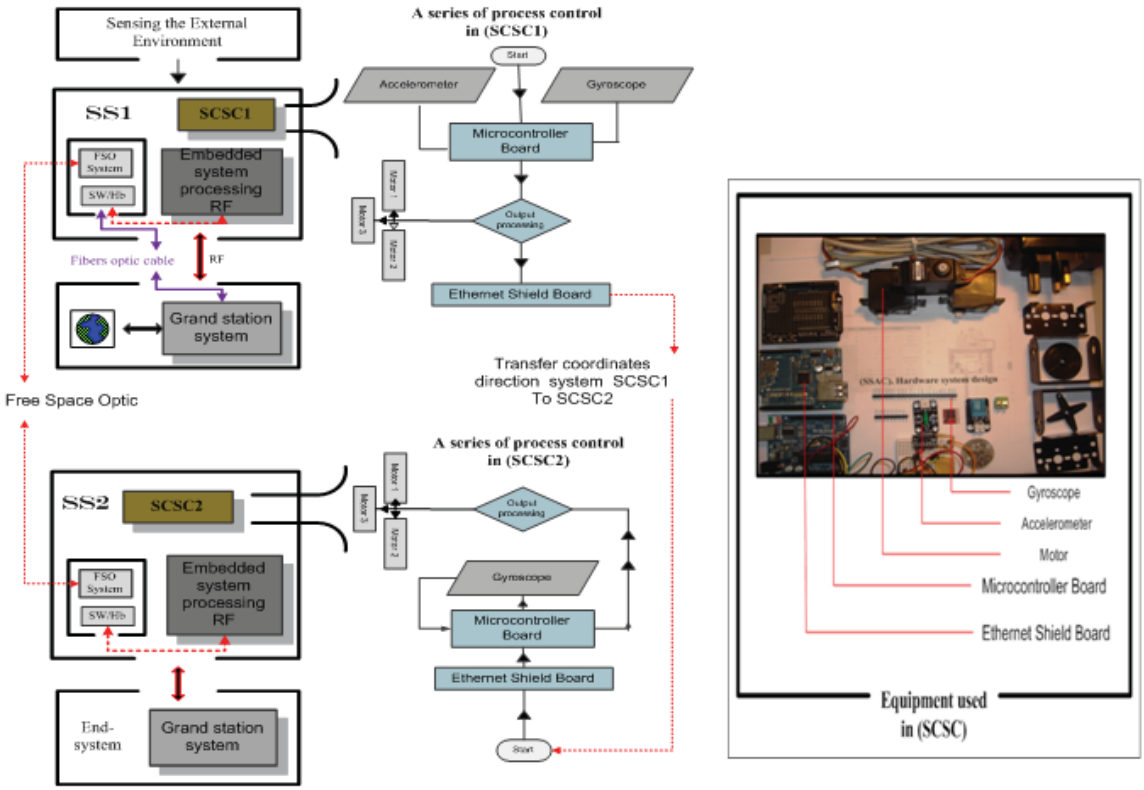

FIGURE 4. SCSC algorithm flowchart in AAPS

Smart Communication System Control (SCSC). The first mission requires transfer variables that influence the system SCPS, from the physical world to the digital world, to transmit the influence of the environmental factors to the communication system. A 3-axis accelerometer with a digital interface that measures the static and dynamic acceleration in all 3-axes [6] is fixed to the SCSC to interact with the vector (R) of the outside force. The vector R can be measured by the accelerometer, to calculate the coordinates of the SCPS, i.e., R_x, R_y, R_z projection of the R vector on the X, Y and Z planes, respectively. The position of R for SCPS that the accelerometer measures are sent to a gyroscope through a micro controller that is compatible with the sensors. The gyroscope is a device for measuring or maintaining system orientation based on the principles of the conservation of angular momentum. The coordinates of the SCPS's position are sent to the gyroscope to be rotated according to any change in the orientation of the rotation axis of a rotating SCPS body, the gyroscope output data is processed by the micro controller, and then the signal is sent to the motors to correct the direction of the SCPS. For converting data about the external movement, C programming language was used to convey the signal from the sensing system to a micro-controller. Figure 4 shows the technical procedures for the mechanism of the system that was used in the SCPS.

After discussing the mechanism of the control system unit and its major components, what remain are a compilation of these components into a single unit and the composition of the essential structure of the system in performing its intended purpose. Figure 5 describes the design of the SCPS system that is used in the AAPS; the design describes the most basic components of the system and the marks numbered to help clarify each component and its location in the system.

2.3. **Structural elements of SCPS.** For a detailed description of the innovation, all components are numbered in Figure 5. The SCPS components are illustrated in Figures

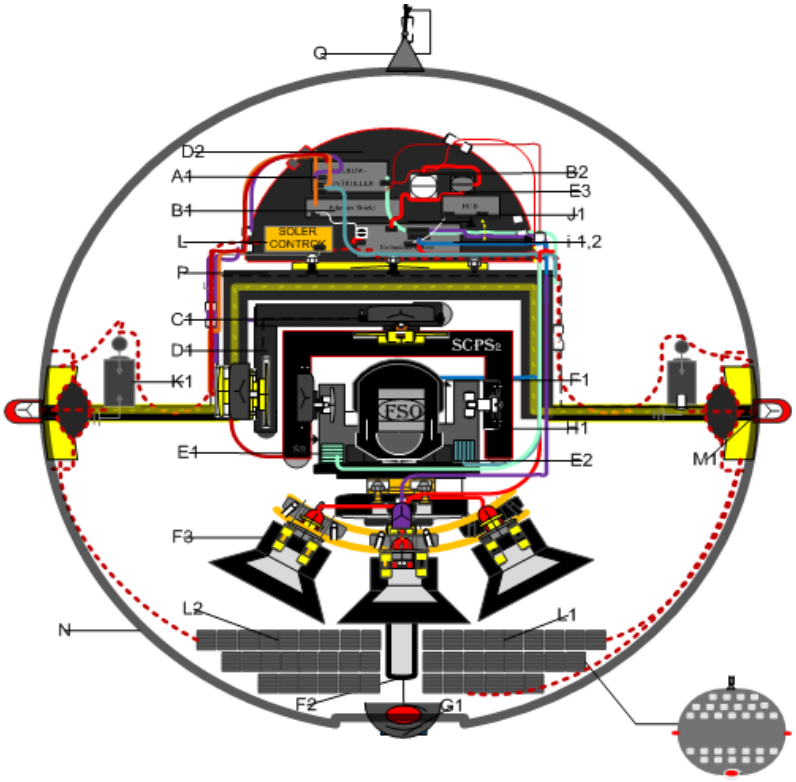

FIGURE 5. Smart communication platform system (SCPS) novel design

4 and 5, including the movement control platform, (N) the transparent plastic ball that constitutes the external shell around the SCPS system to protect it, where the solar cells L1 and L2 are fixed on N. The platform box (D2) contains the control boards at the top level of the SCPS; the GPS described in the (B2) is a space-based system that provides reliable location and time information for the AAPS. GPS sensors with the board shield (E3) have been linked to the micro-controller (A1). (I) is the embedded system hardware with the personal computer memory card international (PCMCIA) – WAN I1 and LAN I2. Figure 5 illustrates the dynamic parts of the sub-platform with 3 motors (C), which are designed to receive the signal that has been sent by the micro-controller and thus organize the movement of the communication system provide (IEEE 802.11a in 5.8 GHz, IEEE 802.11 b/g in 2.4 GHz) and FSO, which has been installed on the platform. The mechanism of FSO performance will be discussed in Section 3.2. The IP camera system (G1) has been installed with D1 for the surveillance area.

The design of the SCPS system that is used in the AAPS is described in Figure 5. The design describes the most essential components of the system.

The control system for solar cell L, which are fixed inside D2, the charger batteries K1, and K2 are fixed as well outside D2 and inside the N, respectively. The parts of the dynamic platform D1, are installed on the predicate link P, to link the SCPS with the N, the alarm lamps M1, and M2 are fixed outside N; it ring connecting for cord Q to tie N to the balloons.

To transfer the influence of the environmental factors on the communication system, a sensing system should be fixed in the SCPS. The 3-axis accelerometer (E1) with digital interfaces is used and is fixed to D1 to interact with the vector of the outside force (R). The vector R can be measured by the accelerometer, to calculate the coordinate of the SCPS, i.e., R_x, R_y, R_z projections of the R vector on the X, Y, and Z planes, respectively. The position of R for the SCPS, which the accelerometer measures, is sent to a gyroscope through the micro-controller that is compatible with the sensors. The 3-axis gyroscope (E2) is a device for measuring or maintaining orientation. The coordinates of the SCPS position are sent to the gyroscope to be rotated in response to that change, the gyroscope output data is processed by the micro-controller, and the signal is then sent to the motors to correct the SCPS direction. For converting the external sensing of the event, C programming language was used to translate the signal from the sensing system to a micro-controller. Figure 4 describes the technical procedures for the mechanism of the system that is used in the SCPS. This section has described the mechanism of the control system unit and its major components, as a compilation of these components in a single unit as well as the composition of the essential structure of the system in performing its intended purpose.

3. **Design and Simulation.**

Free-space optical FSO communication can provide high optic connectivity in the 'last mile' for solving the bottleneck problem. FSO is also being seriously investigated as a means for establishing high-bandwidth links for other applications, including inter-satellite communication, space-borne Internet, and battlefield communications [7,8]. Free space optics has emerged as a promising technology for next generation wireless broadband networks [9,10]. FSO networks began to be considered as a viable candidate for broadband networks for the next-generation [11,12], and for solving the last mile bottleneck problem. Generally, FSO is designed to be appropriate to work on fixed platforms. However, in our case, it was used to be convenient to work on mobile platforms. This development was accompanied in performance, to exceed the challenges; e.g., the narrow beam property of the FSO link is another problem that makes it hard to

keep the link strongly connected; proposed here about the possibility of control over the determinants that hinder the use of FSO.

3.1. **SCPS system design.** In order to discover and track the performance of the communication system, and to ensure that the system has the aptitude to revise the angle deviation located in the permitted range, the system has been built via a MATLAB simulator, and based on the SCSC algorithm that appears in Figure 4.

Figures 6 and 7 illustrate the MATLAB design for SCSC in SCPS units, and showing its components, i.e., the PID controller, accelerometer, gyroscope, servo motor and theta angle determination subsystem that were discussed earlier in Figure 4. Simulation tracker controllers are given in a comparative form in Figure 7.

3.2. **FSO system design.** The receiver at the SCPS nodes has a specific minimum sensitivity at a given data rate, and the task is to ensure that the received power stays

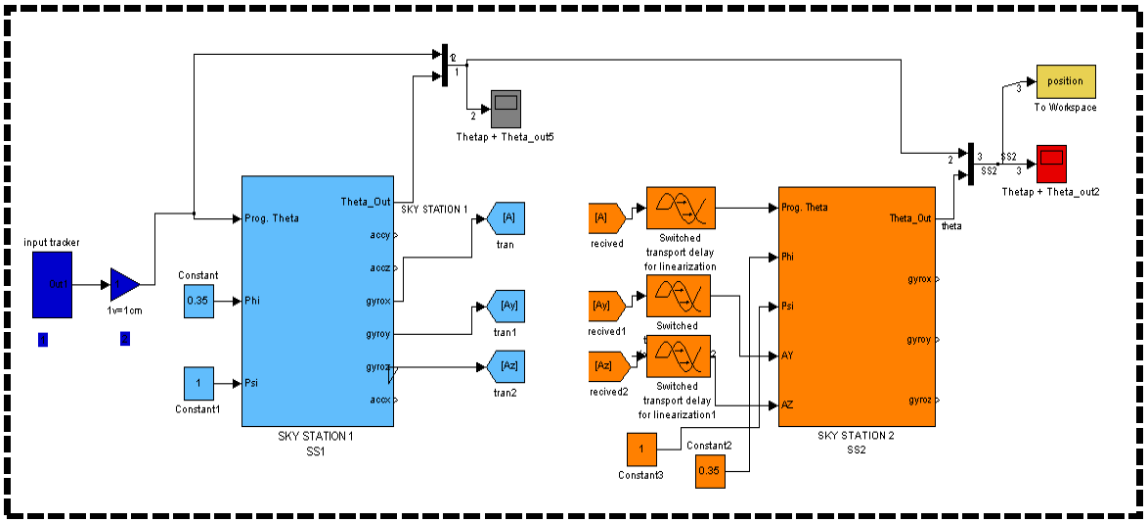

FIGURE 6. Controller design of the SS1 and SS2 using MATLAB simulator

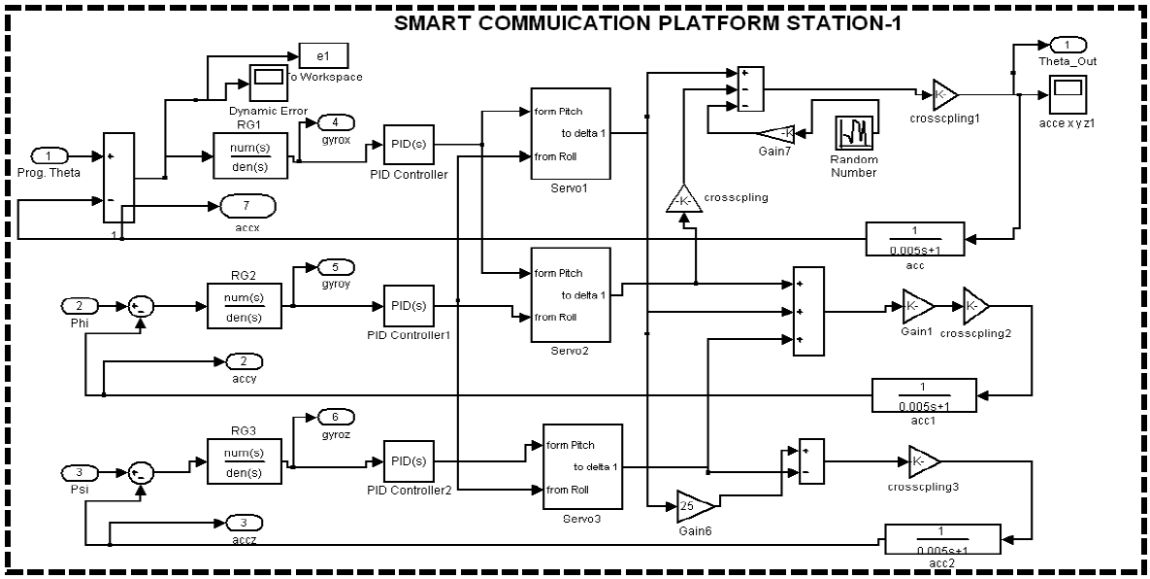

FIGURE 7. Design of the position controller for SCPS unit models using the MATLAB simulator

above the lowest sensitivity to guarantee reliable operation within the system. However, an FSO link parameter is related to the fact that the loss of the medium (air) between the transmitter and receiver can vary in time due to the impact of weather. Therefore, it is important for an FSO system to consider weather conditions. In our experiment, system analysis is evaluated under clear weather conditions with (3 dB/km) attenuation effects. The block diagram of a proposed hybrid network RF/FSO systems [13-15] integrated with an FSO system is shown in Figure 2. Figure 8 shows the essential concept and devices that have been used in designing the bidirectional system between SCPS nodes. The transmission part includes a Pseudo-Random Bit Generator, NRZ Pulse Generator, CW Laser, and Mach-Zehnder Modulator, while the APD photo-detector and Low-Pass Gaussian Filter were used in the receiver part.

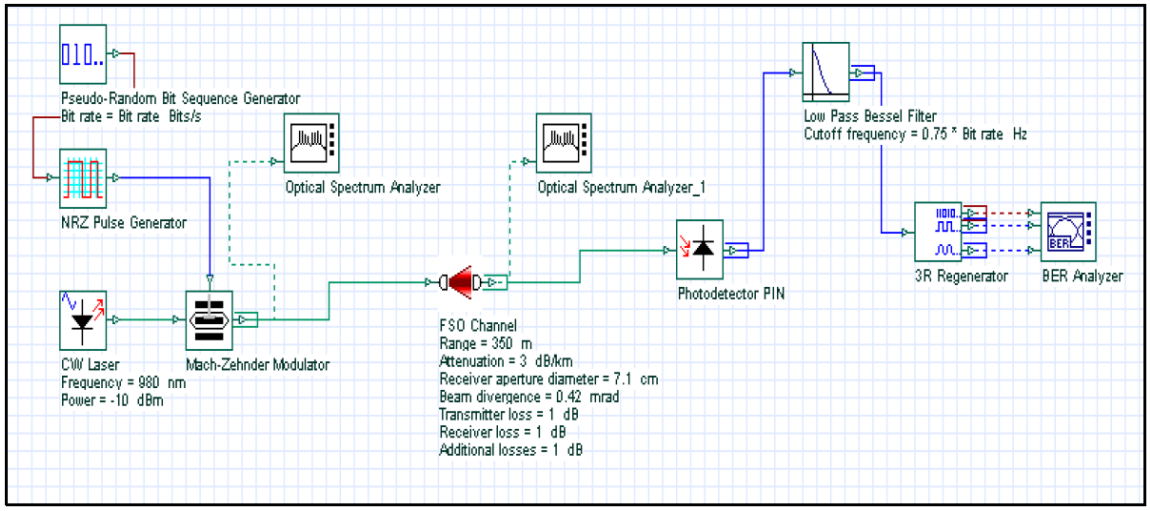

FIGURE 8. The essential components used in designing the FSO system

FSO system parameters were set according to the typical industry values to simulate the real environment as closely as possible, as [16] it provides reliable and secure point-to-point connectivity of up to 350 meters.

Based on Table 1, the aperture angle between the two SCPS nodes is simulated using optical simulator software "*Optisystem*^{TM}" from Optiwave. However, there is a tradeoff between FSO parameters, such as transmit power, wavelength, link range, and the impact of weather conditions. The quality of the received signal greatly depends on the conditions of the free space channel and the stability of the designed system. There is a point, which is necessary to mention where studies have been done using a range of angles of deviation (shown in Table 1) to examine the performance of the SCPS, and to achieve a maximum range of operation.

TABLE 1. The FSO channel parameter

Dynamic range	**Attenuation for Clear Weather**	**Receiver aperture diameter**	**Transmitter aperture diameter**	**Transmitter loss**	**Transmit power**	**Frequency**	**Angle divergence/ Values range**
350 m	3 db/km	7.5 cm	5 cm	1 db	−10 db	785 nm	(0.2, 0.3, 0.4, 0.42, 0.45) mrad

3.3. **Approach connectivity justifications for both mobile FSO nodes.** In order to trace and maintain the line of sight between mobile platform nodes, which suffers from disruption in the balance due to random motion in the lower layers of the atmosphere, as a result of environmental conditions, the study requires the use of an unconventional approach for the handling of these constraints. It is not commonly accepted using free space optic technology as an alternative option in the mobile platforms for increasing the QoS due to limitations of the beam divergence angle, but the concept is bold and could be considered as a high-accuracy stable platform for broadcast of data packets to their destination. One of the critical points to be contemplated when using FSO is the beam divergence angle, especially in the field of our search, for the fact that the FSO is installed on a mobile platform. Continuity of data flow, and being BER-acceptable, will depend on the beam divergence angle for the line of sight, and the fact that the FSO has a small divergence angle depending on the product specifications in use. In our experiment, to verify the performance two FSO devices were used one to send the laser beam and the other to receive the distorted beam from movements in the artificial simulation program. In order to evaluate the performance of SCPS and address the divergence angle of direction within the limits of acceptable divergence, Figure 9 shows the most significant factors used to evaluate the limits of the expected beam angle deviation.

This model describes the angle formed on a spherical body for SCPS. Part A shows the θ angle created by the narrow divergence beam via the theta angle, which will be tested later and indicates the restrictions that have been formed by this angle. Positive or negative theta ($\pm 1/2\theta$) angles are the acceptable restrictions in the mobility of the system proposed. In this case, it requires that both systems adapt and adjust the rotational velocity of the movement, before exceeding the limits of the arc length angle for a narrow divergence beam. Part B in Figure 9 describes the state of trace movements between SCPS1 and SCPS2 and describes the state of trace movements between both systems.

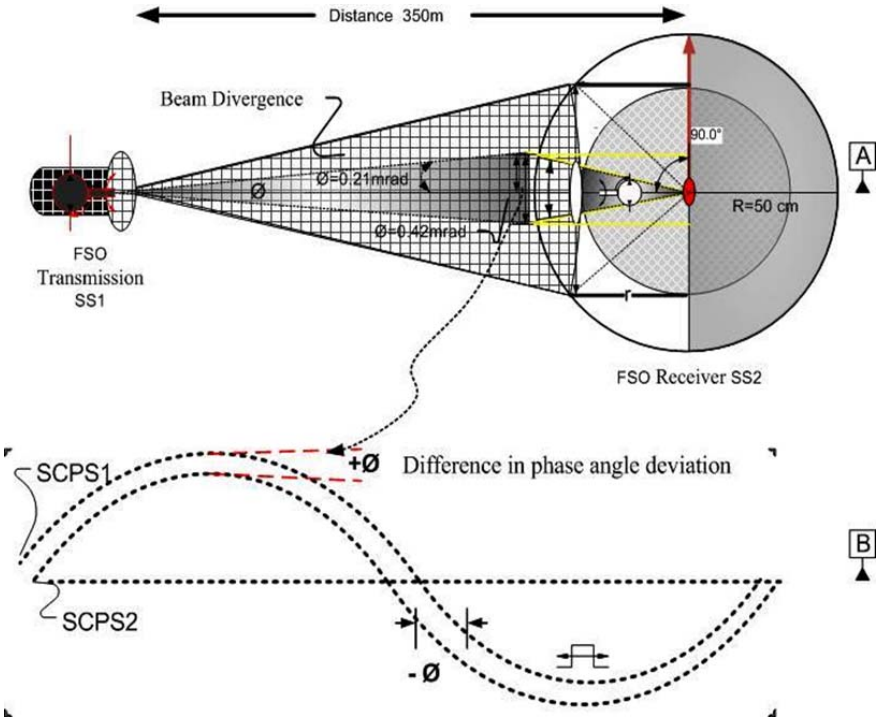

FIGURE 9. Limits of arc length angle for a narrow beam divergence angle

Determinants of half-theta angles ($\pm 1/2\theta$) are the parameters on which the SCPS moves, and decrease the angle value depending on the performance speed of the two systems in synchronized processing to modify the direction of the coordinates; which leads to a decrease in the BER. In fact, this concept is an important point in this research.

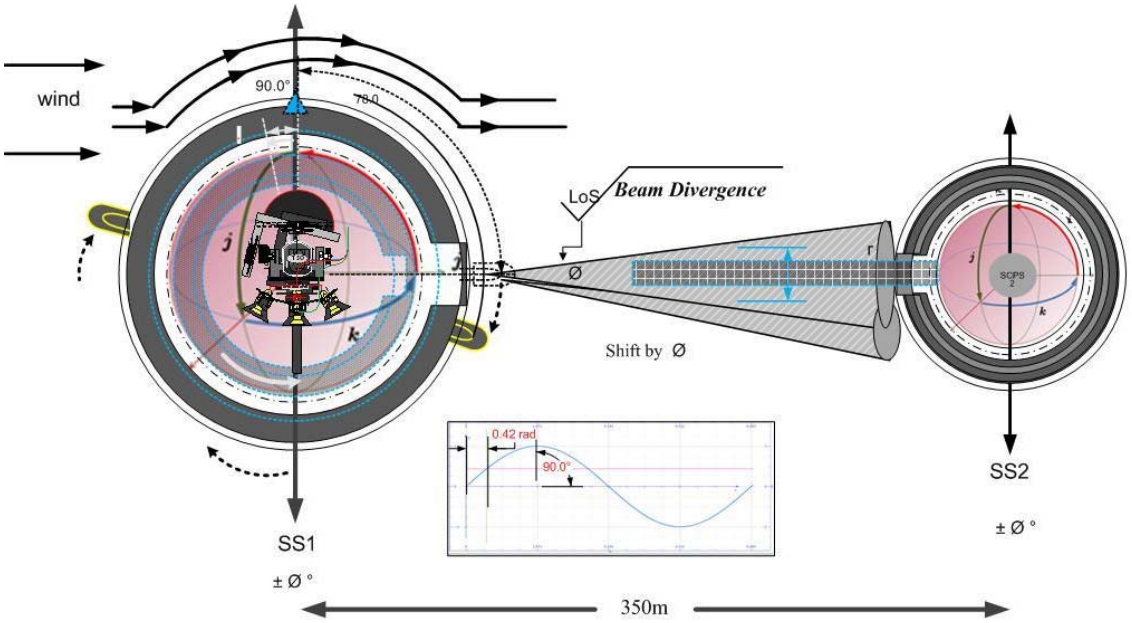

FIGURE 10. The behavior of response systems

Critical behavior of the two systems to address the angle of deviation before exceeding the acceptable limits was discussed previously. Figure 10 displays the mechanism of performance by both systems to decrease the angle of divergence. As discussed earlier, SS2 have tracked the movement of SS1 and revised the angle of deviation before exceeding the limits of the aperture. Figure 10 shows the performance mechanism of both systems within the aperture angle limitation, as an environmental factor affects the outer surface of the spherical body. Control system of SCPS1 senses the new coordinates of the position and tries to maintain the stability of the system, the current coordinates of the body sent to SS2 to change the coordinates simultaneously with the movement of SS1, within the limits of the aperture angle.

4. Results and Discussion.

4.1. **Practical test.** In this section, we present the components of the system mentioned before, in order to ensure the performance of the accelerometer in 3-axes, where an ADXL 345 sensor has measured the environmental factors. Figure 11 shows the deviation of the system by an angle of 45° toward the x-axis in three directions.

The angles of inclination can be calculated using Equations (1)-(3). The experimental system parameters are based on [6].

$$\text{(Sa)possession vector in 3-axis} = \begin{cases} \theta = \tan^{-1}\left(\dfrac{Sa\,x,out}{\sqrt{Sa^2y,out+Sa^2z,out}}\right) & (1) \\ \psi = \tan^{-1}\left(\dfrac{Sa\,y,out}{\sqrt{Sa^2x,out+Sa^2z,out}}\right) & (2) \\ \varphi = \tan^{-1}\left(\dfrac{\sqrt{Sa^2x,out+Sa^2y,out}}{Sa\,z,out}\right) & (3) \end{cases}$$

θ is the angle between the horizon and the x-axis of the (Sa), ψ is the angle between the horizon and the y-axis of Sa, and φ is the angle between the gravity vector g and the z-axis. In the primary position of 0 g on the x- and y-axes and 1 g on the z-axis, all calculated angles would be 0°. The values of x, y and z that were used in previous equations can be obtained from the output readings of the accelerometer.

The consequences of the performance of SAPS for sensing the external environmental changes are illustrated in Figures 11(a)-11(d). In Figure 11, the x-axis represents the measurement of time (0.5) in seconds and the y-axis represents the pulse signal in Figure 11(a). The accelerometer measured sensitivity in the direction of the x-axis, for the y- and z-axes, in illustrations (b), and (c), respectively. (d) defines a 3-axis sensing system. The line with the arrow in the diagrams shows the launch of the movement until the end of the time period of 20-40 seconds. Table 2 indicates the experimental parameters.

4.2. **Simulation experimental results.** Assessing the performance of SCPS requires the following procedures:

Step I: *Extracting the highest permissible deviation angle that can be handled by the FSO; realizing this condition will use a range of deviation angles until the major proportion of the BER is reached.*

Step II: *Adopting the condition of the first phase in the FSO channel configuration designed by "Optisysm^{TM}" simulation program, and experimenting with performance according by altering the angle deviation and correlation with the BER.*

Step III: *Adopting the expected results of the second phase as an influential condition in performance of the SCPS via matlab. These results will be discussed later.*

The first phase has been verified previously. Accordingly, the discussion here will focus on the second phase, focusing specifically on beam divergence; the divergence angle has

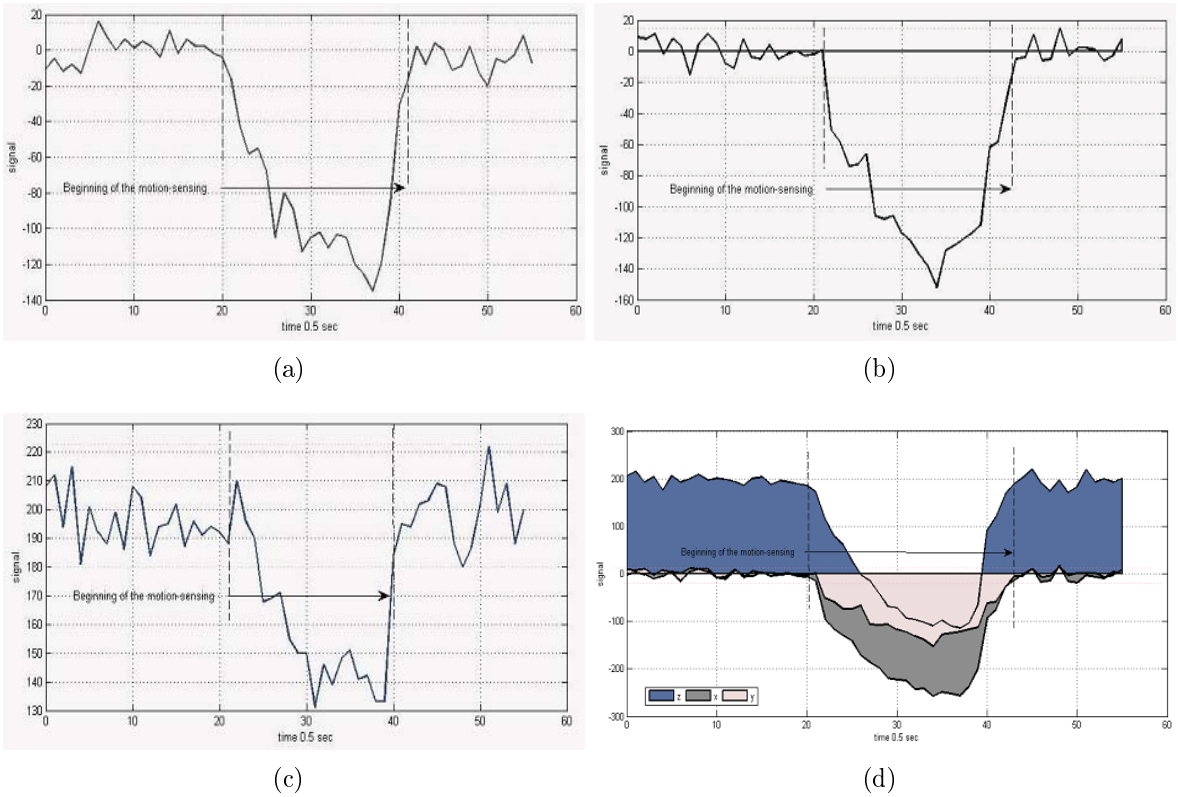

FIGURE 11. Sensing of movement toward the axes

TABLE 2. System parameters

Parameter	Values
Supply voltage range for accelerometer (Acc)	2.0 V to 3.6 V
Sensitivity at (x, y, z) out	256 LSB/g (last significant bit)
Apply voltage range for Acc	2.0 V to 3.6 V
Time movement Experimental	20-40 sec
Y axis – delay time for Acc	0.5 sec
X axis – account numbers	−300 to 300

been obtained depending on the BER in different situations via the optical simulator software "*Optisystem*^{TM}". To estimate and analyze the signal received by the BER analyzer, the optical simulator software used a visualizer, which allows the user to calculate and display the bit error rate of an electrical signal automatically. Figures 12(a) and 12(b) illustrate the BER in the eye time window. Eye pattern is a technique that provides an aggregation of signal measurement information, narrow aperture eye pattern, which makes it more difficult to differentiate between the ones and zeros in the signal and which helps us to evaluate the quality of the received signal.

The discussion will be during the second phase, where the focus is on the beam divergence; the divergence angle has been obtained depending on the BER in different situations via "*Optisystem*^{TM}". To estimate and analyze signals received by the BER analyzer used in "*Optisysm*^{TM}", the visualizer allows the user to calculate and display the bit error rate of an electrical signal automatically. Figures 12(a) and 12(b) illustrate the BER in the eye time window; the eye pattern is a technique that provides an aggregation of signal measurement information, a narrow aperture eye pattern, which leads to more difficulties in differentiating between the ones and zeros in the signal, and which helps us to evaluate the quality of the received signal. The performance of the system was characterized by referring to the BER and eye pattern. For the purpose of analysis the results, should focus on the jitter deformation in eye window receive signal in both cases. The eye pattern for 0.2 and 0.42 mrad as shown in Figures 12(a) and 12(b) clearly shows that the distortion winning eye and narrow aperture eye pattern generated in 0.42

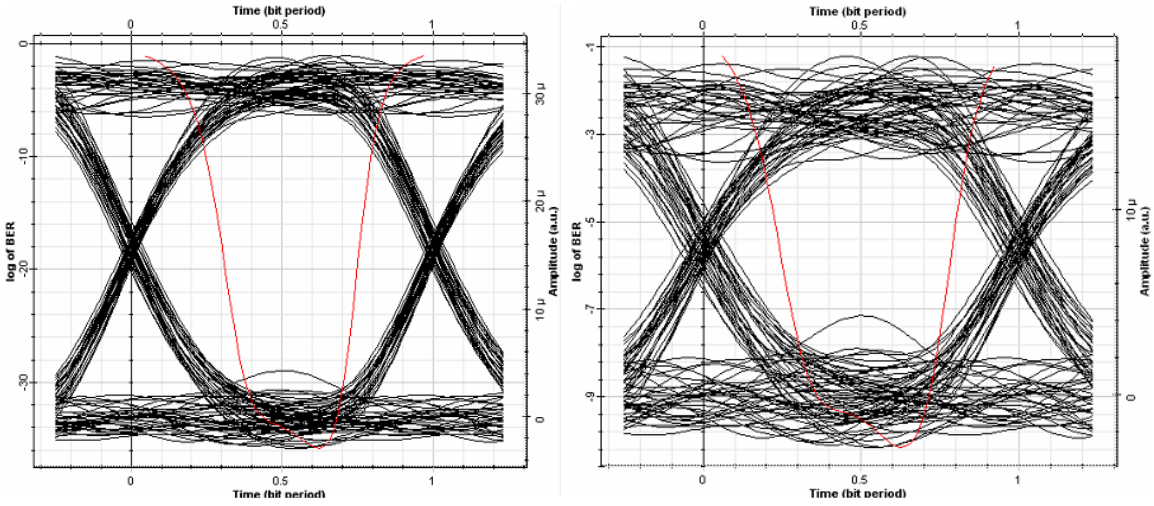

(a) Eye diagram at 0.2 mrad (b) Eye diagram at 0.42 mrad

FIGURE 12. Min BER: at 0.2 and 0.42 mrad

is more than that with 0.2 mrad, which in turn would lead to increasing the proportion of BER.

Experience of the performance test by changing the FSO channel configuration continued until an unacceptable BER was reached.

As we observe in Figure 13 and the margin table, the decision instant is implemented at the 0.59375 bit-period. Accumulated jitter led to more losses in BER, causing more difficulty in distinguishing between ones and zeros in the data signal.

The jitter was executed for the same situation as in Figures 12(a) and 12(b). We conclude from this that any increment for beam divergence increases distortion jitter and narrows the eye pattern; this, in turn, leads to an unacceptable BER close to the $10e^{-9}$.

Table 4 shows the correlation between beam divergence angles vs. minimum BER; therefore, any increase in divergence angle value, on the other hand, causes an increase in the BER. Thus, it can be concluded that the value of 0.42 mrad is considered the minimum acceptable angle of beam deviation that can be adopted.

TABLE 3. Results of the test deflection angle at 0.45 mrad

Max. Q Factor	5.61588
Min. BER	9.77596e-009
Eye Height	2.41423e-006
Threshold	2.55067e-006
Decision Inst.	0.59375

4.3. **Performance test for SCPS.** In order to verify previous concepts, the results are extracted through the second stage, which in turn determines the effectiveness of SCPS performance in the third phase. The following Figures 14, 15 and 16 represent the verification of the stability performance; these figures present a model for the real-time experiment using Real-Time Workspace, which is provided with the MATLAB environment. In order to control the SCPS attitude, it is necessary to know the behavior of the SCPS guidance and stability. Specifically, we need to know the system's reaction to each direction change when supplied with varying angle. The angle was established in initial testing to be nearly identical to the change of direction for SCPS, which is a result of the

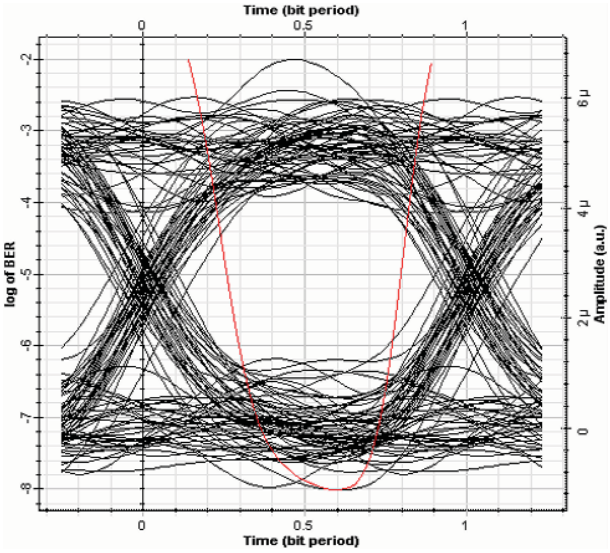

FIGURE 13. Min BER: at 0.45 mrad

TABLE 4. Correlation between the beam divergence and acceptable value for BER

Analysis	**Beam divergence $\theta = 0.2$ mrad**	**Beam divergence $\theta = 0.3$ mrad**	**Beam divergence $\theta = 0.4$ mrad**	**Beam divergence $\theta = 0.42$ mrad**	**Beam divergence $\theta = 0.45$ mrad**
Min. BER	4.10497e-063	5.11401e-024	1.09621e-011	2.36875e-010	9.77596e-009
Acceptable	Acceptable value	Acceptable value	Acceptable value	Acceptable value	Unacceptable value. BER greater than $10e^{-9}$

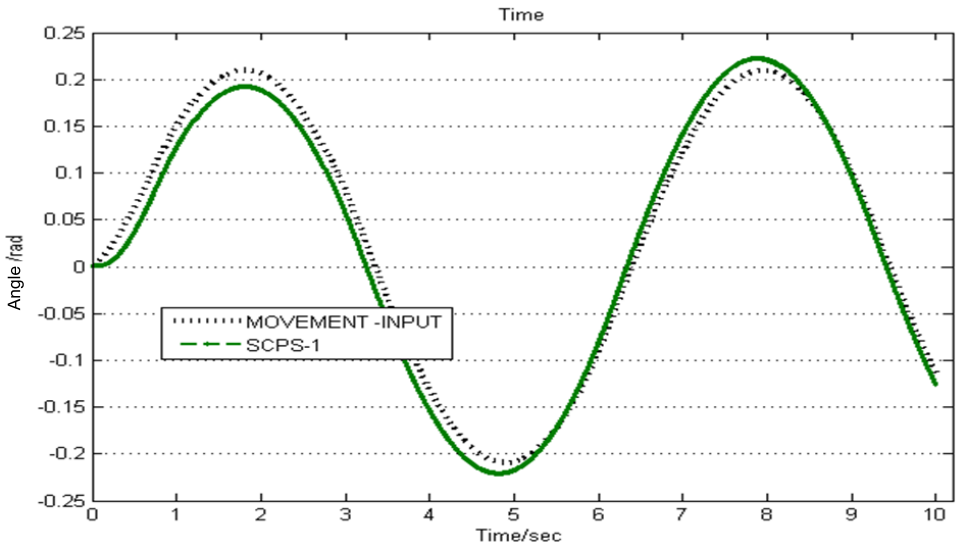

FIGURE 14. SCPS1 behavior and response to movement

impact of external factors and will be affected by the winds. Figures 14 illustrates how the SCPS reduces the gap between its current location and the successive deviation angle, which changes according to the factor influencing movement input.

The output of the SCPS1 procedure algorithm will represent as the second sine wave in Figure 15; SCPS1 sends its current position in the form of (a θ angle) to the second node. In this case, SCPS2 is modifying the direction of the deviation angle for its current location based on new entries that were sent from SCPS1. The mechanism of the algorithm in an SCSC2 enabled SCPS2 to modify its direction and track the movement of SCPS1 constantly. This behavior of procedure appears in the third wave signal of the same figure.

Figure 16, a close-up of Figure 15, shows the time logarithm in the first seconds, signal behavior when the limitation of the initial angular velocity movement will be around the x axis is set to be $\pm 1/2\theta = 0.21$ rad. The parameters of this movement are related to samples per period = 2 * pi/(Frequency * Sample time). The block diagram of SCPS1 control system motion position was directed through a source of sine wave signal input that is processed using the SCSC that traces the input signal in 3-dimensions; this algorithm appeared in Figure 4 previously.

In Figure 16 the angle of phase difference between the two systems is shown. In fact, it represents the proportion of deviation from the line of sight between the two systems SCPS1 and SCPS2; It is axiomatic this deviation is subject to the determinants of movement that are $(\pm 1/2\theta) = 0.21$ mrad, so the output of difference deflection angle between systems can be expressed as:

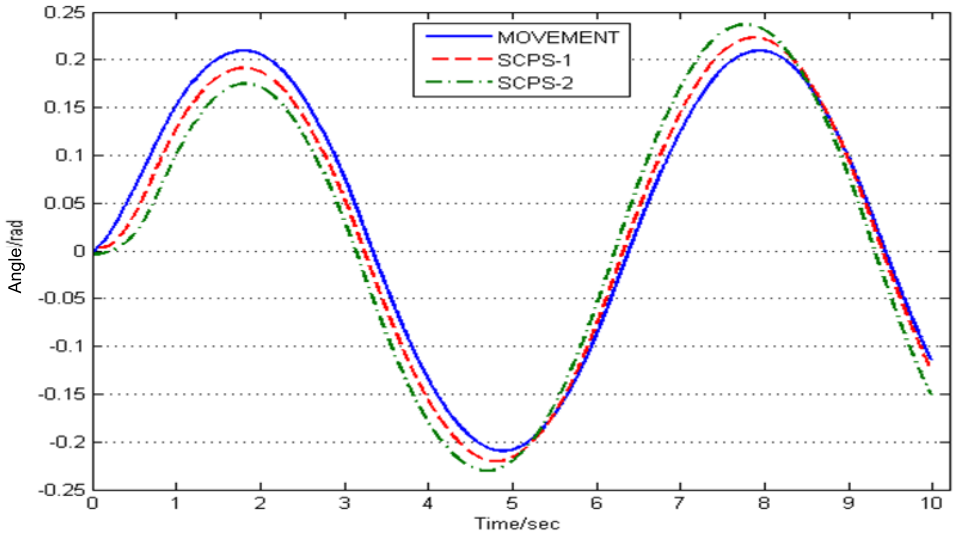

FIGURE 15. Behavior of the two systems' movement

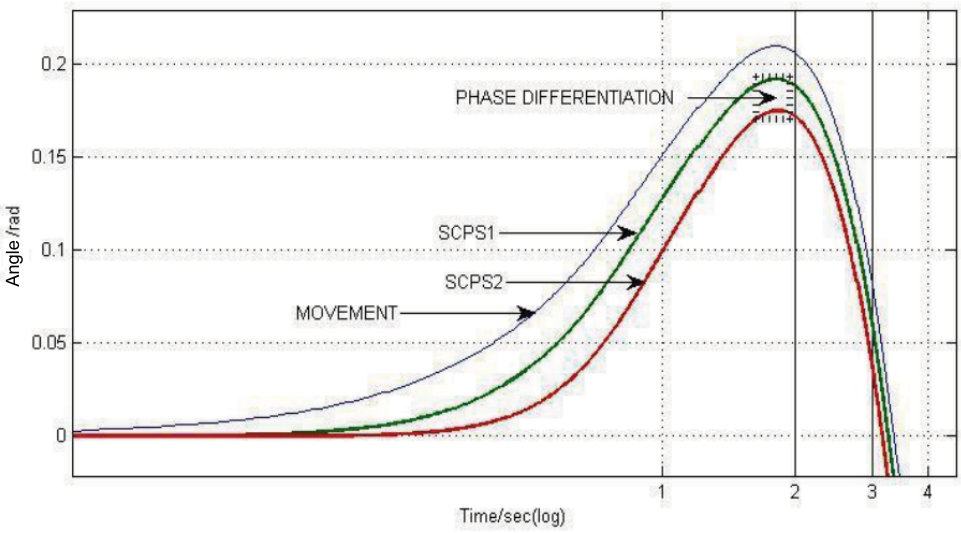

FIGURE 16. Behavior of the two systems and the phase of differentiation

Difference deflection angle (θDd),

$$\underset{-0.21\leq\theta\leq 0.21}{Limitations\,\theta Dd} = |\theta|SCPS1 - |\theta|SCPS2$$

The results appear in Figure 17, which illustrates the behavior of the phase differentiation between the two systems SCPS1 and SCPS2 that should be within permitted deviation restrictions.

Allow us to now scrutinize the behavior of the curve. It appears that θDd does not exceed the limits of the constraint; therefore, it is approving that the SCPS performance response to modify the direction of θ angle deviation for both systems within the limitation of the restrictions condition.

The above concepts lead us to the following fact:

The performance effectiveness for both SCPS systems to achieve stability condition creates a LoS between the mesh nodes deployed.

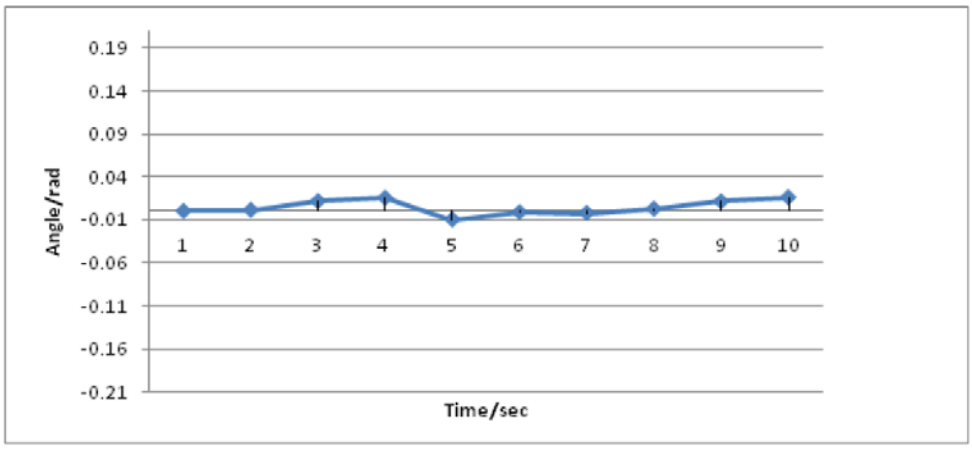

FIGURE 17. Phase differentiation between the two systems

5. **Motivation and Result Merits.** The main advantages of the approaches proposed are to increase and support the performance of communication systems between the nodes deployed, which are distinguished by the achievement highly accurate LoS sight between the nodes deployed. Thus, realization of this concept will lead to the ability to cover the largest number of users and promoting the quality of services through the use of FSO. This feature is to support the broadband capacity for transfer data from a low-level performance through the use of Wi-Fi, to the high level performance through the use of FSO. The purpose of highlighting the qualities and verification, we refer to the following projects according to [17]. For the Emergency Broadband Access Network Using Low-Altitude platform (EBAN), one of the challenges that the EBAN project faced was a problem in the fluctuation of the balloon due to winds. In the EBAN project, the use of ropes to stabilize the blimp against the strong winds increased the weight payload. In fact, the substantive merit of SCPS demonstrated effectiveness in achieving stability against environmental effects, such as a wind, and has been proven through results shown in Figure 13.

According to [17], which examined the statistical characteristics of the wireless channel in sky mesh for stabilization of communication quality, the channel quality is quickly changed due to the swinging of balloon nodes in the wind; and the received signal strength indicator (RSSI) and swing strength of the balloon mesh nodes are measured. When the angle rate is more than 0.1 rad/s, the standard deviation RSSI becomes more than 5 dB, and it is 12 dB if it is more than 0.2 rad/s. Moreover, it will be less than or equal to 2 dB in the case of it being less than 0.05 rad/s. Eventually, [18] is reached, when the x-axis angle rate of the communication equipment increases, the standard deviation of RSSI in the inter-balloon communication increases. On the ability of [18] to increase the reliability of signal transmission between network nodes, we believe that the results of the response SCPS less than 0.21 mrad, as shown in Figure 17, are sufficient to clarify the facts above, which require high reliability of the LoS between the nodes deployed to achieve stability in the quality of communication.

6. **Conclusion.** The results of the experimental simulation proved that this newly proposed subtraction technique on a hybrid RF-FSO successfully achieves its objectives. The performance effectiveness for both systems to achieve stability condition has been achieved.

These promising results prompted the researchers to investigate the feasibility of the use of FSO systems in aerial altitude platform stations to support QoS.

A homogenous mesh network (RF-FSO) was used to enhance high QoS in the 'last-mile'. The novelty of a smart communication platform system (SCPS) is capable of reaching stability in low-level space; therefore, using the FSO in mobile platforms is possible. Hence, it will enhance the deployment of mesh network nodes, which will help solve the 'last-mile' problem in isolated areas. Through these facts and the outcomes obtained, it can be concluded that the 'last-mile' communication performance achieved high efficiency with lower costs, which is the eventual objective of this research.

REFERENCES

[1] P. A. H. Organization, *Management of Dead Bodies in Disaster Situations (D. of & H. Assistance, Trans.) PAHO Cataloguing in Publication*, Area on Emergency Preparedness and Disaster Relief, Washington, USA, 2004.

[2] The Balloon Association, *BALLOON GAS Facts, Figures, Safe Handling and Legislation, Educating, Promoting, Informing*, http://www.balloon.co.uk/Nabas%20gas%20info.pdf, 2007.

[3] C. R. Lee, *Aerial Command and Control Utilizing Wireless Meshed Networks in Support of Joint Tactical Coalition Operations*, 2005.

[4] C. J. Fisher, Using an accelerometer for inclination sensing, *Analog Devices*, TRANZEO Wireless Technology Inc., 2010.

[5] Y. Shibata, Y. Sato, N. Ogasawara and G. Chiba, A disaster information system by ballooned wireless adhoc network, *International Conference on Complex, Intelligent and Software Intensive Systems*, Bradford, United Kingdom, pp.299-304, 2009.

[6] T. Tsuzuki and C. Fisher, Oversampling technique to improve ADXL345 output resolution, *Analog Devices AN1063 an Application Note*, 2010.

[7] J. P. Dodley, D. M. Britz, D. J. Bowen and C. W. Lundgren, Free space optical technology and distribution architecture for broadband metro and local services, *Proc. of SPIE*, vol.4214, pp.72-85, 2001.

[8] T.-H. Ho, S. Trisno, I. I. Smolyaninov, S. D. Milner and C. C. Davis, Studies of pointing, acquisition, and tracking of agile optical wireless transceivers for free space optical communication networks, *Proc. of SPIE*, vol.5237, pp.147-158, 2004.

[9] C. C. Davis, I. I. Smolyaninov and S. D. Milner, Flexible optical wireless links and networks, *IEEE Communications Magazine*, vol.41, no.3, pp.51-57, 2003.

[10] V. W. Chan, Free-space optical communications, *IEEE/OSA Journal of Lightwave Technology*, vol.24, no.12, pp.4750-4762, 2006.

[11] J. C. Juarez, A. Dwivedi, A. R. Mammons, S. D. Jones, V. Weerackody and R. A. Nichols, Free-space optical communications for next-generation military networks, *IEEE Communications Magazine*, vol.44, no.11, pp.46-51, 2006.

[12] S. Ghosh, K. Basu and S. Das, MeshUp: Self-organizing mesh-based topologies for next generation radio access networks, *Ad Hoc Networks Journal*, vol.5, no.6, pp.652-679, 2007.

[13] S. Vangala and H. Pishro-Nik, Optimal hybrid RF-wireless optical communication for maximum efficiency and reliability, *Proc. of the 41st Annual Conference on Information Sciences and Systems*, Baltimore, MD, pp.684-689, 2007.

[14] D. Wang and A. A. Abouzeid, Throughput capacity of hybrid radio-frequency and free-space-optical (RF/FSO) multi-hop networks, *Proc. of Information Theory and Applications Workshop*, San Diego, CA, pp.3-10, 2007.

[15] H. Izadpanah, T. Elbatt, V. Kukshya, F. Dolezal and B. K. Ryu, High-availability free space optical and RF hybrid wireless networks, *IEEE Wireless Communications*, vol.10, no.2, pp.45-53, 2003.

[16] Prologix Distribution, *GeoDesyFSO*, http://www.prologixdistribution.com/GeoDesyFSO/tabid/236/Default.aspx, 2008.

[17] H. Hariyanto, H. Santoso and A. K. Widiawan, Emergency broadband access network using low-altitude platform, *International Conference on Instrumentation, Communications, Information Technology, and Biomedical Engineering*, Bandung, pp.1-6, 2009.

[18] T. Umeki, H. Okada and K. Mase, Evaluation of wireless channel quality for an ad hoc network in the sky, SKYMESH, *The 16th Asia-Pacific Conference Communications*, Auckland, pp.52-57, 2010.